Journal of Intelligent & Robotic Systems (2020) 98:679–692
https://doi.org/10.1007/s10846-019-01089-9

A novel Robust Adaptive Control Using RFWNNs and Backstepping for Industrial Robot Manipulators with Dead-Zone

Nguyen Xuan Quynh[1,2] · Wang Yao Nan[2] · Vu Thi Yen[1]

Received: 16 May 2018 / Accepted: 23 August 2019 / Published online: 10 December 2019

Abstract
This paper proposes a novel robust adaptive-backstepping-recurrent-fuzzy-wavelet-neural-networks controller (ABRFWNNs) based on dead zone compensator for Industrial Robot Manipulators (IRMs) in order to improve high correctness of the position tracking control with the presence of the unknown dynamics, and disturbances. To deal on the unknown dynamics of the robot system problems, the proposed controller used recurrent-fuzzy-wavelet-neural-networks (RFWNNs) to approximate the unknown dynamics. The online adaptive control training laws and estimation of the dead-zone are determined by Lyapunov stability theory and the approximation theory. In this method, the robust sliding-mode-control (SMC) is constructed to optimize parameter vectors, solve the approximation error and higher order terms. Therefore, the stability, robustness, and desired tracking performance of ABRFWNNs for IRMs are guaranteed. The simulations and experiments performed on three-link IRMs are provided in comparison with fuzzy-wavelet-neural-networks (FWNNs) and proportional-integral-derivative (PID) to demonstrate the robustness and effectiveness of the ARBFWNNs.

Keywords Industrial robot · Unknown dead-zone · Recurrent wavelet fuzzy neural networks · Adaptive control

1 Introduction

In recent decades, Robotic manipulators have been widely used in the variety of industries and much effort has been contributed to the robot manipulators for improving their effectiveness and accuracy significantly too. In fact, robotics are multi- input multi – output (MIMO) non-linear systems. In addition, IRMs usually bear the nonlinear frictions, payload variation, external disturbance and etc. in the working process. Therefore, it is not easy to build a suitable controller without the knowledge of the robotic system. To solve these problems, intelligent controllers based on fuzzy/ neural networks control for IRMs have been proposed. The Fuzzy logic technique is a successful implementation for the approximation of nonlinear systems [1–3]. In [3], Shaocheng Tong and Han-xiong Li proposed a sliding mode controller based on fuzzy technique for nonlinear system. Here, the proposed controller was designed without the knowledge of MIMO system and the rules of fuzzy system were created by using the knowledge of human experts and experience to obtain good control performance over uncertainties. However, this knowledge may not be enough and difficult to build the suitable fuzzy control rules, membership function. To overcome this difficult problem, the adaptive robust fuzzy control system based on neural networks were proposed [4–7]. In [5], the authors propose an adaptive robust control system based on fuzzy neural networks (FNNs) for robotic manipulator. The proposed controller combines the advantage of fuzzy technique with fast learning ability of the neural networks. The updated law of the proposed controller was determined by the Lyapunov stability theorem. Therefore, the robustness and stability of FNNs were improved. The FNNs architectures in [4–7] were not easy to solve for the highly nonlinear system because they were built based on the application of feed – forward neural network. To deal with this problem, the recurrent-fuzzy-neural-networks (RFNNs) was proposed [8–14] by inheriting the advance of FNNs with the recurrent technique. In [9], an adaptive iterative learning control for a nonlinear system is proposed by using the recurrent fuzzy neural network. Here, the unknown

✉ Vu Thi Yen
havi2203@gmail.com

[1] Faculty of Electrical Engineering, Hanoi University of Industry, Hanoi 10000, Vietnam

[2] College of Electrical and Information Engineering, Hunan University, Changsha City, Hunan Province 410082, People's Republic of China

certainty equivalent control system was compensated by the recurrent fuzzy neural network. All parameters of the proposed controller were adjusted based on a Lyapunov like analysis. Thus, the robustness and effectiveness of the RFNNs was guaranteed. In [10], Faa – Jeng Lin, and Po- Huang Shieh proposed a recurrent radian-basic-function (RBF) network based on fuzzy neural network controller to control the position of linear ultrasonic motors. By combining recurrent technique, RBF network, and fuzzy neural network, the learning speed of the proposed control system was significantly improved. In general, the control systems based on neural network have the advantages to control the nonlinear system but they still contain some problems as approximation errors, networks size, and poor convergence. There have been many valued researches that proposed based on the wavelet-neural-networks (WNNs) to deal with the problem of FNNs/NNs. By combining the learning capability of neural networks with the decomposition capability of the wavelet, the WNNs can be converged faster, bigger network size, and smaller approximation errors [13–16]. In [14], the authors proposes a wavelet neural network (WNNs) for farm transmission line deicing robot manipulators. In this controller, the disturbances and unknown dynamic system were approximated by the WNNs and the lumped uncertainty was compensated by using the robust term. The proposed controller improved the smaller tracking errors and guaranteed convergence faster than NNs. Other researches proposed the FWNNs have attracted a lot of attention of researchers. The FWNNs are built based on the inheriting advantage of fuzzy technique with WNNs architecture and some researchers by using FWNNs are proposed [17–19]. In [18], an adaptive robust SMC control system based on the inheriting advantage of fuzzy wavelet neural networks (FWNNs) is proposed for a class of condenser cleaning mobile manipulator to solve the problems of external disturbances and parametric uncertainties. In this proposed control system, the FWNNs is applied to approximate the unknown of robot dynamic and the online learning laws are adjusted by the stability Lyapunov theory. Thus, the proposed control system has successfully improved the convergence speed and approximation errors of robotics. Recently years, one of the important subjects for robotic manipulator that has attracted many researchers is the compensation of dead-zone. In fact, deal-zone is a natural and nonlinear item. To deal with compensation of non-smooth nonlinearities, many researches were proposed [20–22]. In [20], an adaptive neural network is proposed to compensate the dead-zone of the hydraulic system. In this proposed controller, the RBF neural network is applied to identify the dead –zone parameters and a cost function is proposed to provide the best approximation of dead-zone. The parameters of the control system and the dead-zone are easier to calculate.

In this paper, to deal with the problem of compensation dead-zone with the unknown dynamic and external disturbance, an adaptive robust recurrent fuzzy wavelet neural network control based on backstepping technique has been proposed. This proposal combines the advantage of RFWNNs, sliding mode control and backstepping technique. The unknown robot dynamics are approximated by the RFWNNs and the tracking errors are compensated by using the robust term. In addition, all the parameters of the proposed controller are adjusted by the stability Lyapunov theory. Thus, the robustness and effectiveness of ABRFWNNs control system are guarantee.

The paper is organized as follows. The preliminaries are described in Section 2. Section 3 presented control design and Stability Analysis. The simulation and experimental results of three-link industrial robot manipulators are provided in section 4. Finally, section 5 gives concluding remarks.

For the convenience of the reader, the main symbols to be used in this paper are summarized in Table 1.

2 Preliminaries

2.1 Model of robotic manipulators

In this paper, the dynamics of an n- link industrial robot manipulator with external disturbance can be described in the Lagrange equation as following:

$$M_R(\theta)\ddot{\theta} + C_R(\theta,\dot{\theta})\dot{\theta} + G_R(\theta) + F_R(\dot{\theta}) = \tau - \tau_0 \qquad (1)$$

with $\theta = [\theta_1\ \theta_2 \ldots \theta_n] \in R^{n\times 1}$ is the joint position vector, $\dot{\theta} = [\dot{\theta}_1\ \dot{\theta}_2 \ldots \dot{\theta}_n] \in R^{n\times 1}$ is the velocity vector and $\ddot{\theta} = [\ddot{\theta}_1\ \ddot{\theta}_2 \ldots \ddot{\theta}_n] \in R^{n\times 1}$ is the acceleration vector. $M_R(\theta)$expresses the $n \times n$ symmetric inertial matrix. $C_R(\theta, \dot{\theta})$ denotes the $n \times n$ vector of Coriolis and Centripetal forces. $G_R(\theta) \in R^{n\times n}$ denotes the Gravity vector. $F_R(\dot{\theta})$ denotes the $n \times 1$ vector of the frictions.

Table 1 Main symbols used in the paper

Variables	Phyical meaning
$\theta_d, \dot{\theta}_d, \ddot{\theta}_d$	The joint position, velocity, acceleration
$Z_{\theta 1}, Z_{\theta 2}$	The tracking error vector and its derivative
W_{lj}	The weight between output layer and rule layer.
a_{ji}	The dilation parameter
b_{ji}	The translation parameter
$\hat{y}$	The approximation of y function
τ_{smc}	Sliding control term
$\hat{W}, \hat{\mu}, \hat{\upsilon}, \hat{a}, \hat{b}$	Approximate values
$\alpha_w, \alpha_v, \alpha_a, \alpha_b, \alpha_\beta, \alpha_\S, \alpha_D$	Positive adaptation rates
§	Positive scalar control gain

τ_0 expresses the $n \times 1$ vector of the input unknown disturbances. And τ is the $n \times 1$ control input vector of joints torque. For designing controller, several properties of the robot dynamics (1) have been assumed as follows.

- *Property 1:* $M_R(\theta)$ is the $n \times n$ symmetric inertial Matrix and bounded:

$$m_1\|x\|^2 \leq x^T M_R(\theta)x \leq m_2\|x\|^2, \forall x \in R^n \tag{2}$$

With $m_1$and m_2 are known positive constants.

- *Property 2:* $\dot{M}_R(\theta) - 2C_R(\theta,\dot{\theta})$ is skew symmetry matrix, in which

$$x^T\left[\dot{M}_R(\theta) - 2C_R\left(\theta,\dot{\theta}\right)\right]x = 0 \tag{3}$$

- *Property 3:* $C_R(\theta,\dot{\theta})\dot{\theta}$, $G_R(\theta)$ and $F_R(\dot{\theta})$ are satisfied:

$$\begin{aligned}&\left\|C_R\left(\theta,\dot{\theta}\right)\dot{\theta}\right\| \leq C_k\left\|\dot{\theta}\right\|^2, \|G_R(\theta)\| \\ &\leq G_k, \left\|F_R\left(\dot{\theta}\right)\right\| \leq F_k\left\|\dot{\theta}\right\| + F_0\end{aligned} \tag{4}$$

With C_k, G_k, F_k, F_0 are positive constants.

- *Property 4:* $\tau_0 \in R^n$ is the unknown disturbance and τ_0 is bounded as follows:

$$\|\tau_0\| \leq \tau_k, \tau_k > 0 \tag{5}$$

As assumptions in [25], the dead zone function shows in Fig. 1 that is expressed as follows:

$$\begin{aligned}&\tau = D(u) \\ &D(u) = \begin{cases} h_r(u - d_r) \text{ for } u > d_r \\ 0 \text{ for } d_l \leq u \leq d_r \\ h_l(u + d_l) \text{ for } u < d_l \end{cases}\end{aligned} \tag{6}$$

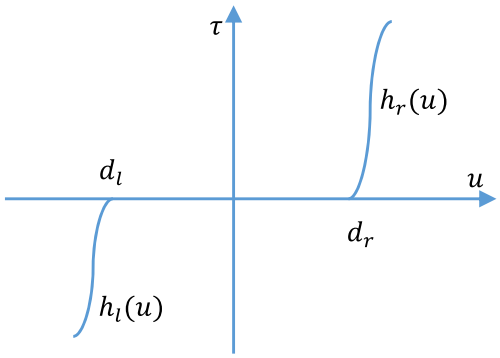

Fig. 1 Dead zone model

Here,

$d_r > 0$, $d_l <$ 0	are unknown constant parameters of dead zone.
$h_l(u)$, $h_r(u)$	are the unknown smooth functions.

Where,

u	is control input before entering the dead zone.
τ	is control input after entering the dead zone.

Therefore (6) can be rewritten as:

$$\tau = D(u) = u - sat_D(u) \tag{7}$$

where the asymmetric saturation function is defined as:

$$sat_D(u) = \begin{cases} d_r \text{ for } u > d_r \\ u \text{ for } d_l \leq u \leq d_r \\ d_l \text{ for } u < d_l \end{cases} \tag{8}$$

2.2 Backstepping controller

The proceeding design of the conventional Backstepping controller is described step by step as follow:

Step 1: Define the tracking error vector $Z_{\theta 1}(t)$ and derivative of $Z_{\theta 1}(t)$ as:

$$Z_{\theta 1}(t) = \theta_d - \theta, \dot{Z}_{\theta 1}(t) = \dot{\theta}_d - \dot{\theta} \tag{9}$$

By using $\dot{\theta}$ as the first virtual control input. Define an intermediate function as:

$$\begin{aligned}&\varphi_{\theta 1}(t) = \dot{\theta}_d + \Omega_{\theta 1} Z_{\theta 1}, \\ &\dot{\varphi}_{\theta 1}(t) = \theta_d + \Omega_{\theta 1}\dot{Z}_{\theta 1}\end{aligned} \tag{10}$$

where $\Omega_{\theta 1} > 0$.

Choose the first following Lyapunov function candidate $L_{\theta 1}$ as:

$$L_{\theta 1}(Z_{\theta 1}(t)) = \frac{1}{2} Z_{\theta 1}^T Z_{\theta 1} \tag{11}$$

The tracking error vector $Z_{\theta 2}(t)$ is define as the follows:

$$Z_{\theta 2}(t) = \varphi_{\theta 1}(t) - \dot{\theta} = \dot{Z}_{\theta 1}(t) + \Omega_{\theta 1} Z_{\theta 1} \tag{12}$$

The time derivative of the Lyapunov function $L_{\theta 1}(Z_{\theta 1}(t))$ is:

$$\dot{L}_{\theta 1}(Z_{\theta 1}(t)) = Z_{\theta 1}^T \dot{Z}_{\theta 1} = Z_{\theta 1}^T (Z_{\theta 2}(t) - \Omega_{\theta 1} Z_{\theta 1}) \tag{13}$$

Step 2: the derivative of tracking error vector $Z_{\theta 2}(t)$ along to time, we have

$$\dot{Z}_{\theta 2}(t) = \dot{\varphi}_{\theta 1}(t) - \dot{\theta} \tag{14}$$

where θ used as the second virtual control input.

Substituting (9, 10, 12, 14) into (1), we have:

$$M_R \dot{Z}_{\theta 2} = M_R \dot{\varphi}_{\theta 1} + C_R \varphi_{\theta 1} - C_R Z_{\theta 2} + G_R + F_R + \tau_0 - \tau \tag{15}$$

Consider the second following Lyapunov function candidate $L_{\theta 2}$ as:

$$L_{\theta 2}(Z_{\theta 1}(t), Z_{\theta 2}(t)) = L_{\theta 1}(Z_{\theta 1}(t)) + \frac{1}{2} Z_{\theta 2}^T M_R Z_{\theta 2} \tag{16}$$

The time derivative of the Lyapunov function $L_{\theta 2}(Z_{\theta 1}(t), Z_{\theta 2}(t))$ is:

$$\dot{L}_{\theta 2}(Z_{\theta 1}(t), Z_{\theta 2}(t)) = Z_{\theta 1}^T (Z_{\theta 2}(t) - \Omega_{\theta 1} Z_{\theta 1}) + \frac{1}{2} Z_{\theta 2}^T \dot{M}_R Z_{\theta 2} + Z_{\theta 2}^T M_R \dot{Z}_{\theta 2} \tag{17}$$

Substituting (15) into (17) and use Property 2, we have:

$$\dot{L}_{\theta 2} = Z_{\theta 1}^T (Z_{\theta 2}(t) - \Omega_{\theta 1} Z_{\theta 1}) + \frac{1}{2} Z_{\theta 2}^T \dot{M}_R Z_{\theta 2} + Z_{\theta 2}^T \left(M_R \dot{\varphi}_{\theta 1} + C_R \varphi_{\theta 1} - C_R Z_{\theta 2} + G_R + F_R + \tau_0 - \tau \right)$$

$$\dot{L}_{\theta 2} = Z_{\theta 1}^T Z_{\theta 2}(t) - Z_{\theta 1}^T \Omega_{\theta 1} Z_{\theta 1} + \frac{1}{2} Z_{\theta 2}^T \left(\dot{M}_R - 2C_R \right) Z_{\theta 2} + Z_{\theta 2}^T (y + \tau_0 - \tau)$$

$$\dot{L}_{\theta 2} = Z_{\theta 1}^T Z_{\theta 2}(t) - Z_{\theta 1}^T \Omega_{\theta 1} Z_{\theta 1} + Z_{\theta 2}^T (y + \tau_0 - \tau) \tag{18}$$

with

$$y = M_R \dot{\varphi}_{\theta 1} + C_R \varphi_{\theta 1} + G_R + F_R \tag{19}$$

To continue our design, the adaptive control law is proposed as:

$$\tau = y + \Omega_{\theta 2} Z_{\theta 2} + Z_{\theta 1} + \tau_0 \tag{20}$$

With $\Omega_{\theta 2} > 0$

Substituting (20) into (18), we have:

$$\dot{L}_{\theta 2} = -Z_{\theta 1}^T \Omega_{\theta 1} Z_{\theta 1} - Z_{\theta 2}^T \Omega_{\theta 2} Z_{\theta 2} \leq 0 \tag{21}$$

Since (21), $\dot{L}_{\theta 2}(Z_{\theta 1}(t), Z_{\theta 2}(t)) \leq 0$, $\dot{L}_{\theta 2}(Z_{\theta 1}(t), Z_{\theta 2}(t))$ is a negative semidefinite function, $\dot{L}_{\theta 2}(Z_{\theta 1}(t), Z_{\theta 2}(t)) \leq \dot{L}_{\theta 2}(Z_{\theta 1}(0), Z_{\theta 2}(0))$. if $Z_{\theta 1}(t)$, $Z_{\theta 2}(t)$ are bounded with $t > 0$. By defining $\epsilon(t) = Z_{\theta 1}^T \Omega_{\theta 1} Z_{\theta 1} + Z_{\theta 2}^T \Omega_{\theta 2} Z_{\theta 2}$ so $\epsilon(t) \leq \dot{L}_{\theta 2}(Z_{\theta 1}(t), Z_{\theta 2}(t))$ and integrate the $\epsilon(t)$ with respect to time as follows:

$$\int_0^t \epsilon(\zeta) d\zeta \leq L_{\theta 2}(Z_{\theta 1}(t), Z_{\theta 2}(t)) - L_{\theta 2}(Z_{\theta 1}(0), Z_{\theta 2}(0)) \tag{22}$$

Because $L_{\theta 2}(Z_{\theta 1}(0), Z_{\theta 2}(0))$ is a bounded function, and $L_{\theta 2}(Z_{\theta 1}(t), Z_{\theta 2}(t))$ is nonincreasing and bounded, we have:

$$\lim_{t \to \infty} \int_0^t \epsilon(\zeta) d\zeta < \infty \tag{23}$$

2.3 Structure of RFWNNs

The proposed RFWNNs are the integration of FWNNs with the recurrent structure. The structure of the RFWNNs is expressed in Fig. 2, which contains m input variables, n number of rule nodes, p output nodes and it includes four layers.

Input Layer (Layer 1): Within this layer, $x = x_1, x_2, \ldots, x_m$ are the input signals. The input values are moved directly to the following layer.

Membership Layer (Layer 2): Every node which describes the terms of corresponding linguistic variable, performs a fuzzy membership function in this layer. The local feed-back unit using the actual time part is added to this present layer. The membership layer output would be represented as:

$$x_{ji}(t) = x_i(t) + \upsilon_{ji} \Psi(x_i(t - T)) \tag{24}$$

where the membership function $\Psi(x_i(t-T))$ denotes the time delay value of $\Psi(x_i(t))$ via an interval T and υ_{ji} is the recurrent weight. $\Psi(x_i(t))$ and $\Psi(x_i(t-T))$ are computed as follows:

$$\Psi(x_i) = e^{-a_{ji}^2 \left(x_i - b_{ji} \right)^2} \tag{25}$$

$$\Psi\left(x_{ji}\right) = e^{-a_{ji}^2 \left(x_{ji} - b_{ji} \right)^2} \tag{26}$$

with a_{ji} is the dilation parameter and, b_{ji} is the translation parameter.

Rule Layer (Layer 3): Each neuron through the rule layer is characterized as a rule and it out prerequisite matching of a rule. The AND operator is used to compute the outputs as follows.

$$\mu_j\left(x_{ji}\right) = \prod_{i=1}^m \omega_{jk} \Psi_j\left(x_{ji}\right) \tag{27}$$

where ω_{jk} is assumed to be unity presents the weight between both the membership layer and the rule layer. The fuzzy wavelet basic function is constituted as follows:

$$\xi_j\left(x_{ji}\right) = \mu_j\left(x_{ji}\right) . \prod_{i=1}^m £_{ji}(x_{ji}) \tag{28}$$

where is the wavelet basis function and could be determined as follows:

$$\xi_j\left(x_{ji}\right) = \prod_{i=1}^m б_j(x_{ji}) \tag{29}$$

where is the Mexican hat wavelet function.

Output Layer (Layer 4): in this layer, every node describes the output linguistic variable, and it will be calculated as follows:

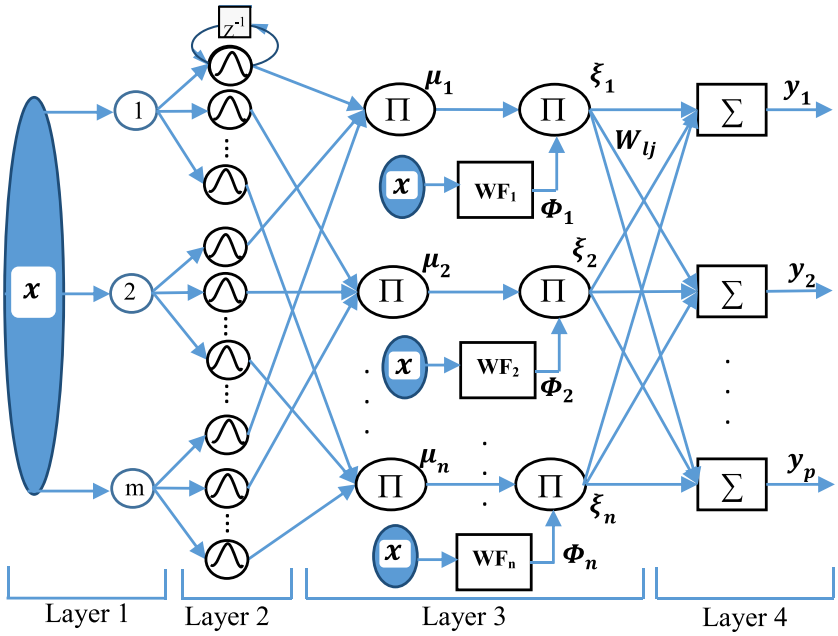

Fig. 2 Structure of a four layer RFWNNs

$$y_l = \sum_{j}^{n} W_{lj}\xi_j(x_{ji}) \tag{30}$$

with W_{lj} is the weight between output layer and rule layer.

The RFWNNs outputs (30) could be expressed in the vector method as follows:

$$y(x,\upsilon,a,\mathrm{b},W) = \left[y_1,y_2,\ldots,y_p\right]^T = W^T\mu(x,\upsilon,a,\mathrm{b}) \tag{31}$$

with

$$\begin{aligned}
&x = [x_1,x_2,\ldots,x_m]^T \in R^{m\times 1},\\
&y = \left[y_1,y_2,\ldots,y_p\right]^T \in R^{p\times 1},\\
&\upsilon = [\upsilon_{11},\upsilon_{12},\ldots,\upsilon_{1m},\ldots,\upsilon,\upsilon_{n2},\ldots,\upsilon_{nm}\,]^T \in R^{mn\times 1};\\
&a = [a_{11},a_{12},\ldots,a_{1m},\ldots,a_{n1},a_{n2},\ldots,a_{nm}]^T \in R^{mn\times 1};\\
&\mathrm{b} = [\mathrm{b}_{11},\mathrm{b}_{12},\ldots,\mathrm{b}_{1m},\ldots,\mathrm{b}_{n1},\mathrm{b}_{n2},\ldots,\mathrm{b}_{nm}\,]^T \in R^{mn\times 1},\\
&\mu(x,\upsilon,a,\mathrm{b}) = [\mu_1,\mu_2,\ldots,\mu_n]^T \in R^{n\times 1};\\
&W = \begin{bmatrix} W_{11} & W_{12} & \ldots & W_{1n}\\ W_{21} & W_{22} & \ldots & W_{2n}\\ \vdots & \vdots & \ddots & \vdots\\ W_{p1} & W_{p2} & \ldots & W_{pn}\end{bmatrix}^T \in R^{p\times n}
\end{aligned}$$

The RFWNNs have been shown as an approximation. Therefore, through investigating the powerful approximation error, there can exit an optimum RFWNNs to learn the nonlinear dynamic *y(x)* with its optimal parameters:

$$y(x) = W^{*T}\mu^*\left(x,\upsilon^*,a^*,\mathrm{b}^*\right) + y_0(x) \tag{32}$$

Here, W^*, υ^*, a^*, $\mathrm{b}^*$are the optimal values of W, υ, a, b one - to - one, and $y_0(x) \in R^n$ is a vector of approximation error.

- *Assumption 1:* $y_0(x)$ will be bounded as:

$$\|y_0(x)\| \le \Delta y \tag{33}$$

with Δy is the positive real value.

- *Assumption 2:* The norm of optimal RFWNNs parameters are limited by positive real values as follows:

$$\|W^*\| \le \Delta w;\ \|\upsilon^*\| \le \Delta\upsilon;\ \|a^*\| \le \Delta a,\ \|b^*\| \le \Delta b \tag{34}$$

The approximate output value of the RFWNNs is determined as:

$$\hat{y} = \hat{W}^T\hat{\mu}\left(x,\hat{\upsilon},\hat{a},\hat{b}\right) \tag{35}$$

where $\hat{y},\hat{W}^T,\hat{\mu},\hat{\upsilon},\hat{a},\hat{b}$ are respectively the approximate values of the optimal parameters y, W^*, μ^*, υ^*, a^*, b^*.

The RFWNNs are constructed on the basic fuzzy rules, the theory of multi-resolution analysis and the recurrent scheme that wavelet function is included in the resulting parts of the rules. The RFWNNs models have a smaller network scope and a faster training speed in comparison to other structures. This structure is created online by means of simultaneous structure and parameter identification. In this RFWNNs structure, the benefits of recurrent possessions can make RFWNNs appropriate to deal with temporal problems.

3 Control design and shabbily analysis

3.1 Control design

We recommend the RFWNNs to find an adaptive law of the suitable adaptive RFWNNs model that makes control system able to achieve the required approximation errors accuracy.

Architecture of the dead zone compensator is shown in Fig. 3.

To compensate the effects of dead zone. The control input after passing the dead zone can be described in the following form [23]:

$$u = \tau_d + \eta\hat{d}^r + (I-\eta)\hat{d}_l \tag{36}$$

where $\eta = I$ if $\tau_d \geq 0$, $\eta = 0$ if $\tau_d < 0$. The direct control input for robot manipulator can be expressed as follows:

$$\begin{aligned} &\tau = \tau_d + \eta\hat{d}_r + (I-\eta)\hat{d}_l \\ &-E_D\left(\tau_d + \eta\hat{d}_r + (I-\eta)\hat{d}_l\right) \\ &\quad = \tau_d - \widetilde{D}^T \Xi + \widetilde{D}^T \delta \end{aligned} \tag{37}$$

where $\widetilde{D} = D-\widehat{D}, \widetilde{D} = diag\left\{\widetilde{d}_1, \widetilde{d}_2, \ldots, \widetilde{d}_n\right\}$ and $\Xi = [\eta\ I - \eta]^T$ and the modelling mismatch δ satisfies the bound [25].

$$\|\delta\| \leq \sqrt{n} \tag{38}$$

Architecture of the adaptive ABRFWNNs with the unknown dead zone is shown in Fig. 4.

As shown in from Fig. 4, the adaptive control law is characterized as presented below:

$$\tau = \mathcal{Y} + \Omega_{\theta 2} Z_{\theta 2} + Z_{\theta 1} + \tau_{smc} - \widetilde{D}^T \Xi + \widetilde{D}^T \delta \tag{39}$$

where $\mathcal{Y}$ is the approximation of y function, and τ_{smc} is a sliding control term.

By using the RFWNNs control law (39) into (15), we can be rewritten as:

$$M_R \dot{Z}_{\theta 2} = \widetilde{y} - (C_R + \Omega_{\theta 2}) Z_{\theta 2} - Z_{\theta 1} - \tau_{smc} + \widetilde{D}^T \Xi - \widetilde{D}^T \delta \tag{40}$$

with

$$\widetilde{y} = y - \mathcal{Y} = W^{*T}\mu^* - \widehat{W}^T \hat{\mu} + y_0 \tag{41}$$

The parameter errors are defined as: $\widetilde{W} = W^* - \widehat{W}; \widetilde{\mu} = \mu^* - \hat{\mu}; \widetilde{\upsilon} = \upsilon^* - \hat{\upsilon}, \widetilde{a} = a^* - \hat{a}$ and $\widetilde{b} = b^* - \hat{b}$. Thus, Eq. (41) is possible to be rephrased as:

$$\widetilde{y} = W^{*T}\widetilde{\mu} + \widetilde{W}^T \hat{\mu} + y_0 \tag{42}$$

The function $\widetilde{\mu}$ can be expanded in a Taylor series as:

$$\begin{aligned} \widetilde{\mu} &= \left[\frac{\partial \mu_1}{\partial \upsilon}, \frac{\partial \mu_2}{\partial \upsilon}, \ldots, \frac{\partial \mu_n}{\partial \upsilon}\right]_{\upsilon=\hat{\upsilon}} \widetilde{\upsilon} \\ &\quad + \left[\frac{\partial \mu_1}{\partial a}, \frac{\partial \mu_2}{\partial a}, \ldots, \frac{\partial \mu_n}{\partial a}\right]_{a=\hat{a}} \widetilde{a} \\ &+ \left[\frac{\partial \mu_1}{\partial b}, \frac{\partial \mu_2}{\partial b}, \ldots, \frac{\partial \mu_n}{\partial b}\right]_{b=\hat{b}} \widetilde{b} + H\left(\widetilde{\upsilon}, \widetilde{a}, \widetilde{b}\right) \end{aligned} \tag{43}$$

or

$$\tilde{\mu} = Б^T \tilde{\upsilon} + Э^T \tilde{a} + \Gamma^T \tilde{b} + H(\tilde{\upsilon}, \tilde{a}, \tilde{b}) \tag{44}$$

where $\mathrm{H}\left(\widetilde{\upsilon}, \widetilde{\mathrm{a}}, \widetilde{\mathrm{b}}\right) \in \mathrm{R}^{\mathrm{n}}$ is the higher- order term vector:

$$\begin{aligned} Б^T &= \left[\frac{\partial \mu_1}{\partial \upsilon}, \frac{\partial \mu_2}{\partial \upsilon}, \ldots, \frac{\partial \mu_n}{\partial \upsilon}\right]_{\upsilon=\hat{\upsilon}} \in R^{n\times(nm)}; \\ Э^T &= \left[\frac{\partial \mu_1}{\partial a}, \frac{\partial \mu_2}{\partial a}, \ldots, \frac{\partial \mu_n}{\partial a}\right]_{a=\hat{a}} \in R^{n\times(nm)}; \\ \Gamma^T &= \left[\frac{\partial \mu_1}{\partial b}, \frac{\partial \mu_2}{\partial b}, \ldots, \frac{\partial \mu_n}{\partial b}\right]_{b=\hat{b}} \in R^{n\times(nm)} \end{aligned}$$

Substitute (44) into (42), we have:

$$\begin{aligned} \tilde{y} &= \widetilde{W}^T[\,\hat{\mu} + Б^T(\upsilon^* - \hat{\upsilon}) + Э^T(a^* - \hat{a}) \\ &\quad + \Gamma^T\left(b^* - \hat{b}\right)] + \widehat{W}\left(Б^T\tilde{\upsilon} + Э^T\tilde{a} + \Gamma^T\tilde{b}\right) \\ &\qquad + W^{*T}H\left(\tilde{\upsilon}, \tilde{a}, \tilde{b}\right) + y_0 \\ \tilde{y} &= \widetilde{W}^T\left(\hat{\mu} - Б^T\hat{\upsilon} - Э^T\hat{a} - \Gamma^T\hat{b}\right) \\ &\quad + \widehat{W}^T\left(Б^T\tilde{\upsilon} + Э^T\tilde{a} + \Gamma^T\tilde{b}\right) + \omega(x, N) \end{aligned} \tag{45}$$

Where

$\omega = [\omega_1, \omega_2, \ldots, \omega_n]^T \in R^n$ and using (44),

we obtain

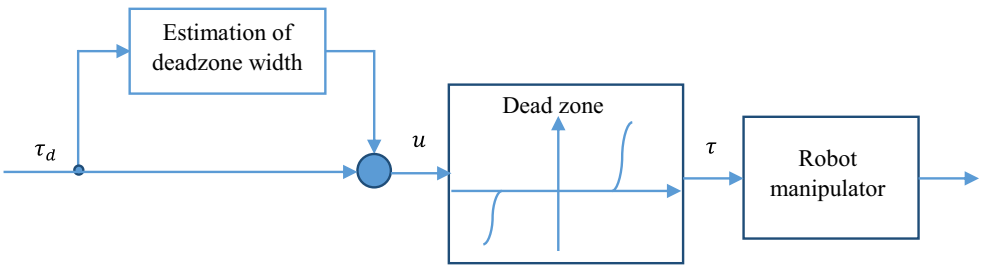

Fig. 3 Adaptive dead zone compensation

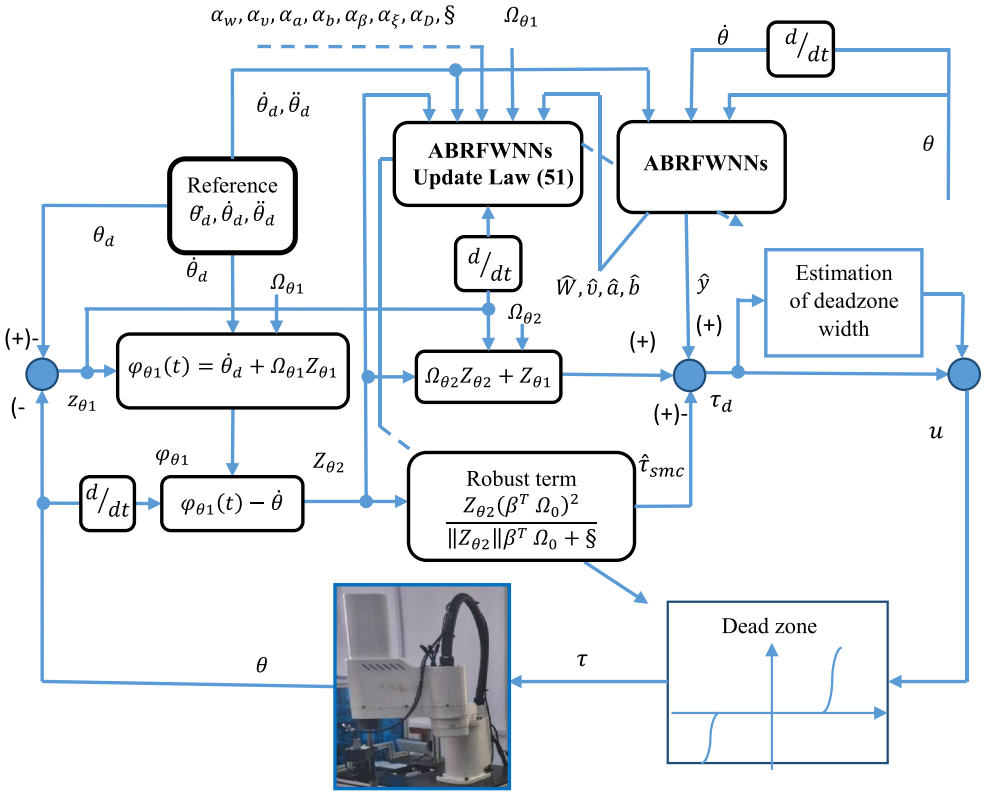

Fig. 4 The block diagram of the adaptive control system

Where
$\omega = [\omega_1, \omega_2, \ldots, \omega_n]^T \in R^n$ and using (44), we obtain

$$\begin{aligned}\omega &= \widetilde{W}^T(Б^T v^* + Э^T a^* + \Gamma^T b^*) + W^{*T} H(\tilde{v}, \tilde{a}, \tilde{b}) + y_0 \\ &= \left(W^{*T} - \widehat{W}^T\right)(Б^T v^* + Э^T a^* + \Gamma^T b^*) + W^{*T}(\tilde{\mu} - Б^T \tilde{v} - Э^T \tilde{a} - \Gamma^T \tilde{b}) + y_0 \\ &= W^{*T}\left(\tilde{\mu} + Б^T \hat{v} + Э^T \hat{a} + \Gamma^T \hat{b}\right) - \widehat{W}^T(Б^T v^* + Э^T a^* + \Gamma^T b^*) + y_0\end{aligned}$$

The bound of ω is determined as:

$$\begin{aligned}\|\omega\| &= \left\|W^{*T}\left(\tilde{\mu} + Б^T \hat{v} + Э^T \hat{a} + \Gamma^T \hat{b}\right) - \widehat{W}^T(Б^T v^* + Э^T a^* + \Gamma^T b^*) + y_0\right\| \\ \|\omega\| &= \left\|(W^{*T}\tilde{\mu} + u_0) + W^{*T}(Б^T \hat{v} + Э^T \hat{a} + \Gamma^T \hat{b}) - \widehat{W}^T(Б^T v^* + Э^T a^* + \Gamma^T b^*)\right\|\end{aligned}$$

Since $\left\|W^{*T} Б^T \hat{v}\right\| \le \left\|W^{*T} Б^T\right\| \|\hat{v}\|$;
$\left\|W^{*T} Э^T \hat{a}\right\| \le \left\|W^{*T} Э^T\right\| \|\hat{a}\|$;
$\left\|W^{*T} \Gamma^T \hat{b}\right\| \le \left\|W^{*T} \Gamma^T\right\| \left\|\hat{b}\right\|$ and $\left\|\widehat{W}^T(Б^T v^* + Э^T a^* + \Gamma^T b^*)\right\| \le \left\|\widehat{W}^T\right\| \|Б^T v^* + Э^T a^* + \Gamma^T b^*\|$

Hence, we can infer:

$$\begin{aligned}\|\omega\| &\le \left\|W^{*T}\tilde{\mu} + y_0\right\| + \left\|W^{*T} Б^T\right\| \|\hat{v}\| + \left\|W^{*T} Э^T\right\| \|\hat{a}\| + \left\|W^{*T}\Gamma^T\right\| \left\|\hat{b}\right\| + \left\|\widehat{W}\right\| \|Б^T v^* + Э^T a^* + \Gamma^T b^*\| \\ \|\omega\| &\le \left[\left\|W^{*T}\tilde{\mu} + y_0\right\|, \left\|W^{*T} Б^T\right\|, \left\|W^{*T} Э^T\right\|, \left\|W^{*T}\Gamma^T\right\|, (\|Б^T v^* + Э^T a^* + \Gamma^T b^*\|)\right]^T \times \left[1, \|\hat{v}\|, \|\hat{a}\|, \left\|\hat{b}\right\|, \left\|\widehat{W}\right\|\right] \\ \|\omega\| &\le \beta^{*T}\Omega_0\end{aligned} \tag{46}$$

where

$$\begin{aligned}\beta^* &= \left[\left\|W^{*T}\tilde{\mu} + u_0\right\|, \left\|W^{*T} Б^T\right\|, \left\|W^{*T} Э^T\right\|, \left\|W^{*T}\Gamma^T\right\|, (\|Б^T v^* + Э^T a^* + \Gamma^T b^*\|)\right]^T; \\ \Omega_0 &= \left[1, \|\hat{v}\|, \|\hat{a}\|, \left\|\hat{b}\right\|, \left\|\widehat{W}\right\|\right]^T\end{aligned}$$

Follow above analysis, a sliding mode control term τ_s is designed by:

$$\tau_{smc} = \frac{Z_{\theta 2}\left(\beta^T\ \Omega_0\right)^2}{\|Z_{\theta 2}\|\beta^T\ \Omega_0 + \S} \tag{47}$$

where § is a positive scalar control gain

$$\dot{\S} = -k_{\S}\S, \S(0) > 0 \tag{48}$$

with

$\beta = [\ \beta_1, \beta_2, \beta_3, \beta_4]^T$ is a bound of vector β^*.

To estimate the sliding control term τ_{smc} we present adaptive term $\hat{\tau}_s$ as:

$$\hat{\tau}_{smc} = \frac{Z_{\theta 2}\left(\hat{\beta}^T\ \Omega_0\right)^2}{\|Z_{\theta 2}\|\hat{\beta}^T\ \Omega_0 + \S} \tag{49}$$

where $\hat{\beta}$ is the estimate of β^*

Applying (45) to (40), yields:

$$\begin{aligned} M_R\dot{Z}_{\theta 2} = {} & \widetilde{W}^T\left(\hat{\mu} - Б^T\hat{\upsilon} - Э^T\hat{a} - \Gamma^T\hat{b}\right) \\ & + \widehat{W}^T\left(Б^T\tilde{\upsilon} + Э^T\tilde{a} + \Gamma^T\tilde{b}\right) + \omega - \tau_{smc} \\ & - (C_R + \Omega_{\theta 2})Z_{\theta 2} - Z_{\theta 1} + \widetilde{D}^T\Xi - \widetilde{D}^T\delta \end{aligned} \tag{50}$$

Based on dynamic model (1), the adaptive control law (39) and the robust sliding compensator (49), the online adaptive update laws of ABRFWNNs, sliding control term parameters can be chosen as:

$$\begin{cases} \dot{\widehat{W}} = \alpha_w\left(\hat{\mu} - Б^T\hat{\upsilon} - Э^T\hat{a} - \Gamma^T\hat{b}\right){Z_{\theta 2}}^T \\ \dot{\hat{\upsilon}} = \alpha_\upsilon\widehat{W}Б^T Z_{\theta 2} \\ \dot{\hat{a}} = \alpha_a\widehat{W}Э^T Z_{\theta 2} \\ \dot{\hat{b}} = \alpha_b\widehat{W}\Gamma^T Z_{\theta 2} \\ \dot{\hat{\beta}} = \alpha_\beta\|Z_{\theta 2}\|\Omega_0 \\ \dot{\S} = -\alpha_\xi\S \\ \dot{\widehat{D}} = \alpha_D\Xi\ {Z_{\theta 2}}^T - \alpha_D k_D\widehat{D}\|Z_{\theta 2}\| \end{cases} \tag{51}$$

here α_w, α_υ, α_a, α_b, α_β, $\alpha_\S$, α_D are positive adaptation rates.

3.2 Stability analysis

Theorem 1 Consider the ABRFWNNs adaptive control law of an n-link robot manipulator represented by (1) is designed in (39), and a sliding control term τ_{smc} is given by (49), and the parameters $\widehat{W}, \dot{\upsilon}, \dot{a}, \dot{\hat{b}}, \dot{\hat{\beta}}, \dot{\S}, \dot{\hat{D}}$, are adjusted by the adaptive algorithm (51). Then the position tracking error and all the system parameters converges to zero.

The Lyapunov function candidate is chosen as follows as:

$$\begin{aligned} L(t) = \frac{1}{2}\Bigg[& {Z_{\theta 1}}^T Z_{\theta 1} + {Z_{\theta 2}}^T M_R Z_{\theta 2} + \frac{1}{\alpha_w}\widetilde{W}^T\widetilde{W} + \frac{1}{\alpha_\upsilon}\tilde{\upsilon}^T\tilde{\upsilon} + \frac{1}{\alpha_a}\tilde{a}^T\tilde{a} \\ & + \frac{1}{\alpha_b}\tilde{b}^T\tilde{b} + \frac{1}{\alpha_\beta}\tilde{\beta}^T\tilde{\beta} + \frac{2}{\alpha_\S}\S + \frac{1}{\alpha_D}tr\left(\widetilde{D}^T\widetilde{D}\right)\Bigg] \end{aligned} \tag{52}$$

The derivative of *V(t)* along to time, we have:

$$\begin{aligned} \dot{L}(t) = {} & Z_{\theta 1}^T(Z_{\theta 2}(t) - \Omega_{\theta 1}Z_{\theta 1}) \\ & + \frac{1}{2}Z_{\theta 2}^T\dot{M}_R Z_{\theta 2} + Z_{\theta 2}^T M_R\dot{Z}_{\theta 2} \\ & - \frac{1}{\alpha_w}\widetilde{W}^T\dot{\widehat{W}} - \frac{1}{\alpha_\upsilon}\tilde{\upsilon}^T\dot{\upsilon} - \frac{1}{\alpha_a}\tilde{a}^T\dot{a} \\ & - \frac{1}{\alpha_b}\tilde{b}^T\dot{\hat{b}} - \frac{1}{\alpha_\beta}\tilde{\beta}^T\dot{\hat{\beta}} + \frac{1}{\alpha_\S}\dot{\S} \\ & - \frac{1}{\alpha_D}tr\left(\widetilde{D}^T\dot{\hat{D}}\right) \end{aligned} \tag{53}$$

Substitute (50) into (53) and using property 2, we obtain

$$\begin{aligned} \dot{L}(t) = {} & -Z_{\theta 1}^T\Omega_{\theta 1}Z_{\theta 1} - Z_{\theta 2}^T\Omega_{\theta 2}Z_{\theta 2} \\ & + Z_{\theta 2}^T\Big(\widetilde{W}^T\left(\hat{\mu} - Б^T\hat{\upsilon} - Э^T\hat{a} - \Gamma^T\hat{b}\right) \\ & + \widehat{W}^T\left(Б^T\tilde{\upsilon} + Э^T\tilde{a} + \Gamma^T\tilde{b}\right) \\ & + \omega - \tau_{smc} + \widetilde{D}^T\Xi - \widetilde{D}^T\delta\Big) \\ & - \frac{1}{\alpha_w}\widetilde{W}^T\dot{\widehat{W}} - \frac{1}{\alpha_\upsilon}\tilde{\upsilon}^T\dot{\hat{\upsilon}} \\ & - \frac{1}{\alpha_a}\tilde{a}^T\dot{\hat{a}} - \frac{1}{\alpha_b}\tilde{b}^T\dot{\hat{b}} \\ & - \frac{1}{\alpha_\beta}\tilde{\beta}^T\dot{\hat{\beta}} + \frac{1}{\alpha_\S}\dot{\S} \\ & - \frac{1}{\alpha_D}tr\left(\widetilde{D}^T\dot{\hat{D}}\right) \end{aligned} \tag{54}$$

Substituting the adaptive algorithm (51) to (54), we have:

$$\begin{aligned} \dot{L}(t) = {} & -Z_{\theta 1}^T\Omega_{\theta 1}Z_{\theta 1} - Z_{\theta 2}^T\Omega_{\theta 2}Z_{\theta 2} + Z_{\theta 2}^T\omega \\ & - Z_{\theta 2}^T\tau_{smc} + Z_{\theta 2}^T\left(\widetilde{D}^T\Xi - \widetilde{D}^T\delta\right) - \widetilde{\beta}^T\|Z_{\theta 2}\|\Omega_0 \\ & - \S - tr\left(\widetilde{D}^T\left(\Xi\ {Z_{\theta 2}}^T - k_D\widehat{D}\|Z_{\theta 2}\|\right)\right) \end{aligned} \tag{55}$$

By using (46) and (49), it becomes

$$\begin{aligned} \dot{L}(t) \le {} & -Z_{\theta 1}^T\Omega_{\theta 1}Z_{\theta 1} - Z_{\theta 2}^T\Omega_{\theta 2}Z_{\theta 2} \\ & - Z_{\theta 2}^T\frac{Z_{\theta 2}\left(\hat{\beta}^T\ \Omega_0\right)^2}{\|Z_{\theta 2}\|\hat{\beta}^T\ \Omega_0 + \S} + Z_{\theta 2}^T\beta^{*T}\Omega_0 \\ & - \widetilde{\beta}^T\|Z_{\theta 2}\|\Omega_0 - \S + tr\left(\widetilde{D}^T Z_{\theta 2}^T(\Xi - \delta)\right) \\ & - tr\left(\widetilde{D}^T\left(\Xi\ {Z_{\theta 2}}^T - k_D\widehat{D}\|Z_{\theta 2}\|\right)\right) \end{aligned}$$

$$\dot{L}(t)\leq -Z_{\theta 1}^{T}\Omega_{\theta 1}Z_{\theta 1}-Z_{\theta 2}^{T}\Omega_{\theta 2}Z_{\theta 2}$$
$$-Z_{\theta 2}^{T}\frac{Z_{\theta 2}\left(\hat{\beta}^{T}\ \Omega_0\right)^{2}}{\|Z_{\theta 2}\|\hat{\beta}^{T}\ \Omega_0+\S}+\hat{\beta}^{T}\|Z_{\theta 2}\|\Omega_0-\S$$
$$+tr\left(\tilde{D}^{T}Z_{\theta 2}^{T}\left(k_D\hat{D}-\delta\right)\right)$$
$$\dot{L}(t)\leq -Z_{\theta 1}^{T}\Omega_{\theta 1}Z_{\theta 1}-Z_{\theta 2}^{T}\Omega_{\theta 2}Z_{\theta 2}$$
$$+\frac{\S\|Z_{\theta 2}\|\hat{\beta}^{T}\ \Omega_0}{\S\|Z_{\theta 2}\|\hat{\beta}^{T}\ \Omega_0+\S}-\S \tag{56}$$
$$+tr\left(\tilde{D}^{T}Z_{\theta 2}^{T}\left(k_D\hat{D}-\delta\right)\right)$$

Since the sum of the last two terms in (56) is always less than zero, we can place the new upper bound on $\dot{L}$

$$\dot{L}\leq -Z_{\theta 1}^{T}\Omega_{\theta 1}Z_{\theta 1}-Z_{\theta 2}^{T}\Omega_{\theta 2}Z_{\theta 2}$$
$$+tr\left(\tilde{D}^{T}Z_{\theta 2}^{T}\left(k_D\left(D-\tilde{D}\right)-\delta\right)\right) \tag{57}$$

By using $tr\tilde{D}^{T}\left(D-\tilde{D}\right)=\left(\tilde{D},D\right)-\|\tilde{D}\|^{2}\leq\|\tilde{D}\|\|D\|-\|\tilde{D}\|^{2}$ and using property 5 into the inequality (57) could be rewritten as follows:

$$\dot{L}\leq -Z_{\theta 1}^{T}\Omega_{\theta 1}Z_{\theta 1}-Z_{\theta 2}^{T}\Omega_{\theta 2}Z_{\theta 2}+\sqrt{n}\|Z_{\theta 2}\|\left\|\tilde{D}\right\|+k_DD_M\|Z_{\theta 2}\|\left\|\tilde{D}\right\|-k_D\|Z_{\theta 2}\|\left\|\tilde{D}\right\|^{2}$$
$$\dot{L}\leq -Z_{\theta 1}^{T}\Omega_{\theta 1}Z_{\theta 1}-Z_{\theta 2}^{T}\Omega_{\theta 2}Z_{\theta 2}+c_0\left\|Z_{\theta 2}\right\|\left\|\tilde{D}\right\|-k_D\|Z_{\theta 2}\|\left\|\tilde{D}\right\|^{2}\Big\| \tag{58}$$

with $c_0=\sqrt{n}+k_DD_M$ we see that to make sure $\dot{L}\leq 0$,

$$-c_0\|Z_{\theta 2}\|\left\|\tilde{D}\right\|+k_D\|Z_{\theta 2}\|\left\|\tilde{D}\right\|^{2}>0 \tag{59}$$

So, if we choose suitable constant vectors k_D, D_M which satisfy (59), $\dot{L}\left(s(t),\S(t),\tilde{W},\tilde{v},\tilde{a},\tilde{b},\tilde{\beta}\right)\leq 0$, $L\left(s(t),\S(t),\tilde{W},\tilde{v},\tilde{a},\tilde{b},\tilde{\beta}\right)$ is a negative semidefinite function, $\dot{L}\left(s(t),\S(t),\tilde{W},\tilde{v},\tilde{a},\tilde{b},\tilde{\beta}\right)\leq\dot{L}\left(s(0),\S(0),\tilde{W},\tilde{v},\tilde{a},\tilde{b},\tilde{\beta}\right)$, if all parameters such as $s(t),\S(t),\tilde{W},\tilde{v},\tilde{a},\tilde{b},\tilde{\beta}$ are bounded with $t>0$. By defining $\epsilon(t)=s^{T}K_ss$ so $\epsilon(t)\leq-\dot{L}(t)$ and integrate the $\epsilon(t)$ with respect to time as follows:

$$\int_0^t\epsilon(\xi)d\xi\leq L\left(s(0),\S(0),\tilde{W},\tilde{v},\tilde{a},\tilde{b},\tilde{\beta}\right)$$
$$-L\left(s(t),\S(t),\tilde{W},\tilde{v},\tilde{a},\tilde{b},\tilde{\beta}\right) \tag{60}$$

Because $L\left(s(0),\tilde{W}_D,\tilde{W}_V,\tilde{W}_g,\tilde{W}_F\right)$ is a bounded function, and $L\left(s(t),\tilde{W}_D,\tilde{W}_V,\tilde{W}_g,\tilde{W}_F\right)$ is nonincreasing and bounded, we have

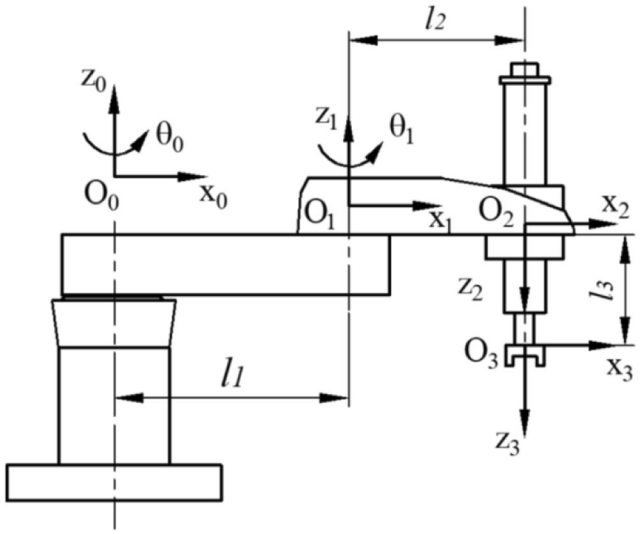

Fig. 5 The model of three-joint IRMs

$$\lim_{t\to\infty}\int_0^t\epsilon(\xi)d\xi<\infty \tag{61}$$

According to Barbalat's Lemma [26], when $\dot{\epsilon}(t)$ is bounded function. It can be shown that $\lim_{t\to\infty}\int_0^t\epsilon(t)dt=0$. From this outcome, we see that, s(t) will converge to zero when $t\to\infty$ and the global stability of the control system for IRMs is assured by the updated law (39).

From the control design analysis, the design procedure of the ABFWNNs control systems can be summarized as follows:

set $\Omega_{\theta 1}$, $\Omega_{\theta 2}$, α_w, α_v, α_a, α_b

Step 1: initial the parameters of the ABRFWNNs $\hat{W},\hat{v},\hat{a},\hat{b},\Psi(x_{ji})$ with random values.

Step 2: Update the ABRFWNNs inputs: $x=\left[\theta^{T},\dot{\theta}^{T},\theta_d^{T},\dot{\theta}_d^{T},\theta_d^{T}\right]^{T}$ and, $\hat{W},\hat{v},\hat{a},\hat{b},\Psi(x_{ji})$ from memory. Calculate the error signal $Z_{\theta 1}$.

Step 3: Calculate the virtual control input $\varphi_{\theta 1}(t)$

Step 4: Calculate the output of the fuzzy rule layer via (27). Then calculate fuzzy wavelet basic function via (28) and (29). Next, calculate the output of the ABRFWNNs via (30).

Step 5: Calculate the output of the ABRFWNNs $\hat{y}$, and the robust term τ_{smc}. Where, the weight parameters are updated as (51).

Step 6: Calculate the control input τ

Step 7: Return to step 3

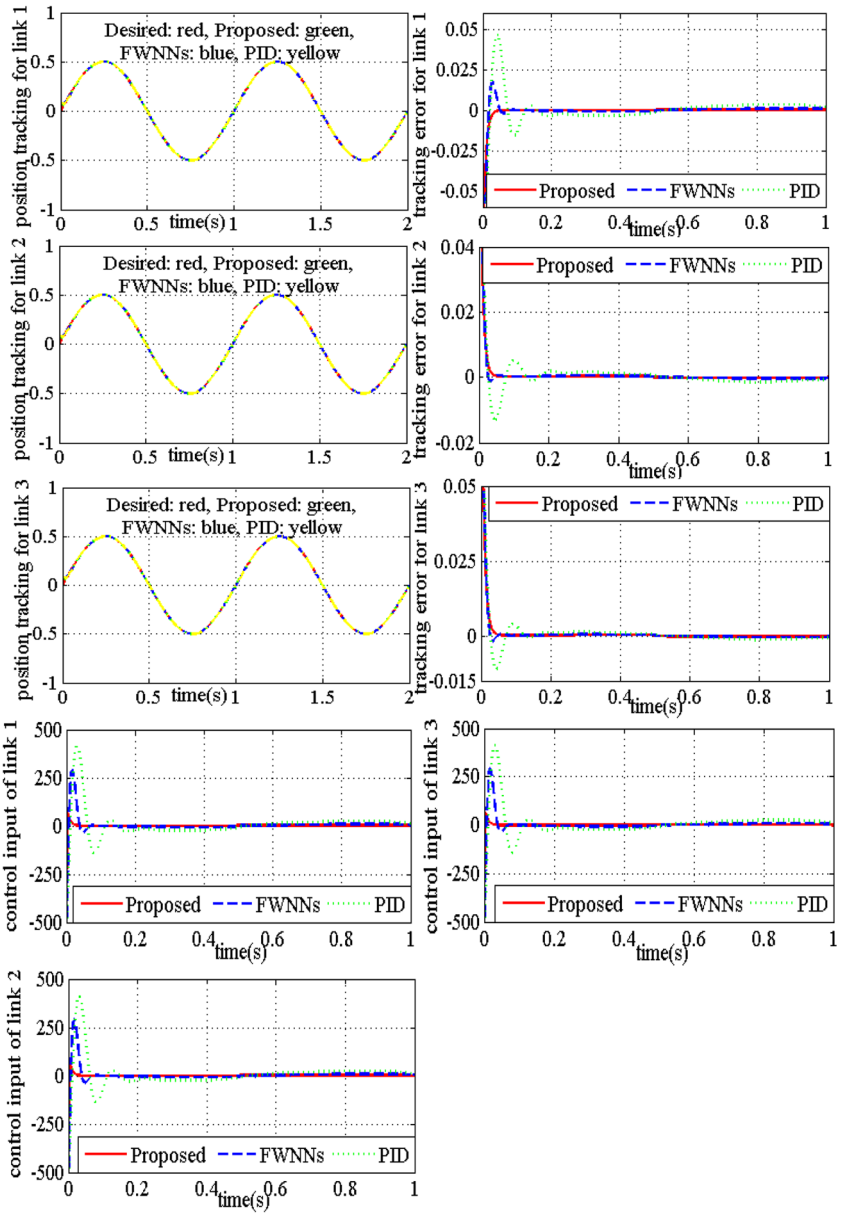

Fig. 6 Simulated results of trajectory, tracking errors, control efforts of FWNNs, PID and the proposed controller

4 Simulation and experimental results

4.1 Simulation results

Here, a three-link IRMs is applied to confirm the efficiency of the suggested control method based on RFWNNs for illustrative purposes. The detailed system parameters of three-link IRMs model (Fig. 5) are given as follows:

$$M = \begin{bmatrix} M_{11} & M_{12} & M_{13} \\ M_{21} & M_{22} & M_{23} \\ M_{31} & M_{32} & M_{33} \end{bmatrix} \quad C = \begin{bmatrix} C_{11} & C_{12} & C_{13} \\ C_{21} & C_{22} & C_{23} \\ C_{31} & C_{32} & C_{33} \end{bmatrix};$$

$$G = \begin{bmatrix} g_1 \\ g_2 \\ g_3 \end{bmatrix};$$

$$M_{11} = l_1^2\left(\frac{p_1}{3} + p_2 + p_3\right) + l_1 l_2 (p_2 + 2p_3)\cos(\theta_2) + l_2^2\left(\frac{p_2}{3} + p_3\right)$$

$M_{12} = -l_1 l_2\left(\frac{p_2}{3} + p_3\right)\cos(\theta_2) - l_2^2\left(\frac{p_2}{3} + p_3\right)$; $M_{13} = M_{23} = M_{31} = M_{32} = 0$; $M_{21} = M_{12}$

$M_{22} = l_2^2\left(\frac{p_2}{3} + p_3\right)$; $M_{33} = p_3$

$C_{11} = -\dot{\theta}_2(p_2 + 2p_3)$; $C_{12} = C_{21}$; $C_{13} = C_{22} = C_{23} = C_{31} = C_{32} = C_{33} = 0$

$$g_1 = g_2 = g_3 = -p_3 g$$

Where p_1, p_2, p_3 are links masses; l_1, l_2, l_3 are links lengths. The parameters of three link IRMs are given as follows:

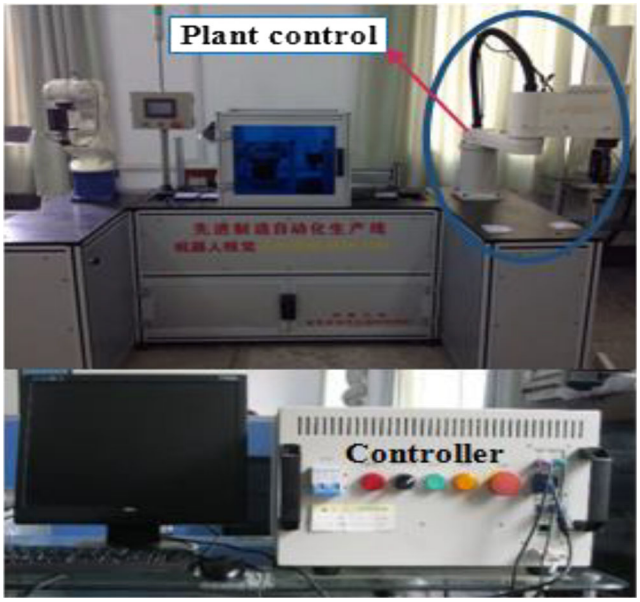

Fig. 7 Experimental control system

$p_1 = 4.2\ (kg), p_2 = 3\ (kg), p_3 = 1.52\ (kg);$

$l_1 = 420\ (mm)$, $l_2 = 380\ (mm)$, $l_3 = 250\ (mm)$; $g = 10(m/s^2)$

The desired joint trajectories of the three link industrial robot manipulator are chosen by: $\theta_d = [\theta_{d1}\ \theta_{d2}\ \theta_{d3}]^T = [\ 0.5\sin(2\pi t)\quad 0.5\sin(2\pi t)\quad 0.5\sin(2\pi t)\ ]^T$;

In addition, external disturbances and friction force in this simulation are selected as following:

$$\tau_0 = \begin{bmatrix} 2\sin(\pi t) \\ 2\sin(\pi t) \\ 2\sin(\pi t) \end{bmatrix}; F(\dot{\theta}) = \begin{bmatrix} 5\dot{\theta}_1 + 0.2sign(\dot{\theta}_1) \\ 5\dot{\theta}_2 + 0.2sign(\dot{\theta}_2) \\ 5\dot{\theta}_3 + 0.2sign(\dot{\theta}_3) \end{bmatrix}$$

The proposed controller parameter values are given as follows:

$$\lambda = diag(6,6,6); K = diag(100,110,100);$$
$$\alpha_w = diag(50,50,50,50,50);$$
$$\alpha_v = \alpha_a = \alpha_b = diag(40,\ldots,40,\ldots,40) \in R^{mp \times mp};$$
$$\alpha_\beta = diag(0.001,0.001,0.001,0.001,0.001);$$
$$\alpha_\varepsilon = 0.1$$

The initial conditions of §and, Ω are selected as follows: $\S(0) = 1$, $\Omega(0) = [1\ 1\ 1\ 1]$

In order to exhibit the superior control performance and effectiveness of the proposed controller, the PID control and FWNNs [24] were examined in the meanwhile. The PID law can be defined as:

$$\tau = K_P e(t) + K_I \int_0^t e(t)dt + K_D \dot{e}(t)$$

Where K_P, K_I, K_D denote proportional, integral and differential gain matrices, respectively, and they are designed by a compromise between the superiority of control performance and the magnitude of the control effort. K_P, K_I, K_D are given as $K_P = diag\ (70,50,60)$, $K_I = diag\ (0.5,0.2,0.5)$, $K_D = diag\ (900, 800,800)$,

In here, the proposed ABRFWNNs is applied to control the IRMs in comparison with the FWNNs [24] and PID. The simulation results of the FWNNs, PID and the proposed ABRFWNNs are shown in Fig. 6. Since the simulated results, we see that, the position tracking of three links with the ABRFWNNs, FWNNs, and PID can be guaranteed, and the tracking errors of the FWNNs, PID and the proposed intelligent controller are converged. However, the proposed intelligent control system converges faster than the FWNNs and PID systems. It means that all updated parameters in the dynamic structure ABRFWNNs and the amount of the rule nodes are adjusted, the approximation capability of the dynamics structure ABRFWNNs is also superior to the FWNNs and PID systems. Moreover, from Fig. 6 it can be observe that, the control force of the suggested RFWNNs is smoother and has smaller oscillation than the FWNNs and PID to attain the requested level of performance when the tracking errors reach the high value.

4.2 Experimental results

Here, we implemented two experimental outcomes to prove the efficiency of the ABRFWNNs controller on a three link robot manipulators. The experimental control system model is presented in Fig. 7.

The first experimental example assumes that 0.5-kg payload is added in the masses of three links IRMs, and all parameters are the same as in the simulation model. The experimental results of joint trajectory, control torques and tracking errors are exposed in Fig. 8. It is noticed that the position tracking of IRMs are still obtained with PID, FWNNs,

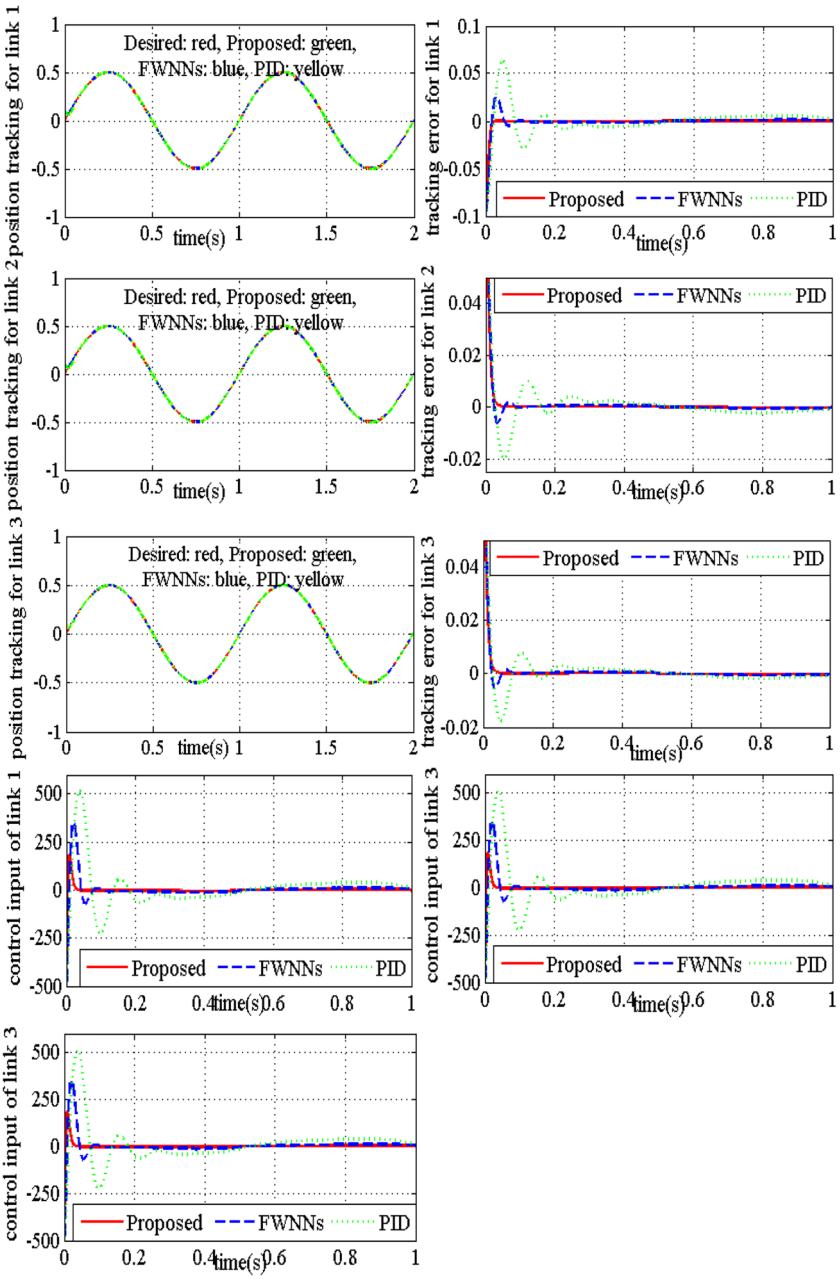

Fig. 8 Trajectory, control efforts and tracking errors of the FWNNs, PID and the proposed control system in the first experimental case

and ABRFWNNs, however the responses and the tracking error norm of the ABRFWNNs are quite better than the FWNNs and PID methods. Furthermore, these results shows that the proposed intelligent controller torques are less and smooth than FWNNs in [24], and PID which still exist the chattering phenomena when a load of manipulators changed. Therefore, the position tracking performance of the recommended ABRFWNNs is better than the FWNNs and PID under parameters variation. It means that due to the dynamic structure, the proposed ABRFWNNs is less sensitive to the parameter variation than the FWNNs and PID.

The second experimental case, the external disturbance $d_e(t)$ is suddenly injected more into control system when the robot is tracking a trajectory. This occurred after the first 0.4 s of the experimental period, and all other parameters are the same as in the simulation model. The external disturbance shapes are expressed as follows:

$$d_e(t) = [\,30\sin(20t) \quad 30\sin(20t) \;\; 30\sin(20t)\,]^T$$

The experimental outcomes of the second case are shown in Fig. 9. According to these results, it is easy to see that, the performance of the proposed ABRFWNNs is just slightly affected, while the performance of PID approach is seriously affected. Therefore, the control performance and robustness

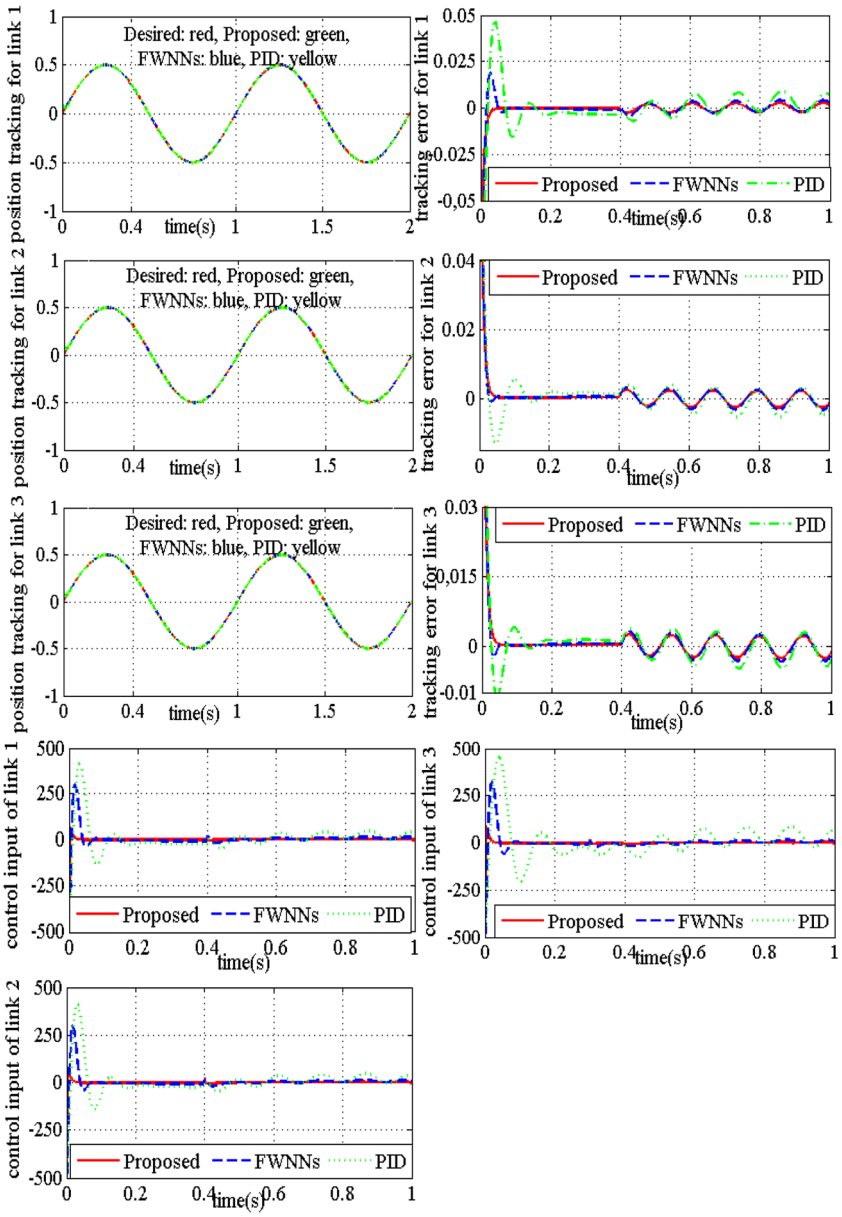

Fig. 9 Trajectory, control efforts and tracking errors of the FWNNs, PID and the proposed control system in the second experimental case

of the proposed ABRFWNNs under external disturbance are better than the FWNNs [24] and PID. It is obvious that the performance of the proposed ABRFWNNs is better than the FWNN and PID system after a period of learning.

5 Conclusions

In the present paper, a robust adaptive controller based on the RFWNNs and backstepping technique has been proposed, and the stability analysis of controller has been proofed. It has been also successfully implemented to control the joints of three-link IRMs for achieving high precision position tracking and compensation dead-zone. By combining the RFWNNs, backstepping technique, and Lyapunov stability theorem, the adaptive control laws are developed to tune all parameters of the network in order to reduce approximation error and improved control performance. In addition, the robust controller is designed to deal with the approximation error, prime parameter vectors and higher order terms in Taylor series. Therefore, the proposed controller proved that this control system could achieve desired tracking performance, the stability and robustness of the closed-loop manipulators system are guaranteed. Simulation and experimental results of a three-links IRMs via the proposed RFWNNs and FWNN, RNFN also have provided in this study to compare and display. The proposed ABRFWNNs control systems can be applied to other systems, such as MMR, AC servo systems, and they can also be applied as a good alternative in the existing industrial robot manipulator control system. This application could require further investigations.

Acknowledgements This work was supported by National Natural Science Foundation of China (Grant nos. 61175075) National Hightech Research and Development Projects (Grant nos. 2012AA112312, Grant nos. 2012AA11004). The authors would like to thank the editor and the reviewers for their invaluable suggestions, which greatly improved the quality for this paper dramatically.

References

1. Wang, L.X.: Stable Adaptive Fuzzy Control of Nonlinear Systems. IEEE Trans. Fuzzy Syst. **1**(2), 46–155 (1993)
2. Tong, S., Chen, B., Wang, Y.: Fuzzy adaptive output feedback control for MIMO nonlinear systems. Fuzzy Sets Syst. **156**, 285–299 (2005)
3. Tong, S., Li, H.X.: Fuzzy Adaptive Sliding – Mode Control for MIMO Nonlinear Systems. IEEE Trans. Fuzzy Syst. **11**(3), 354–360 (2003)
4. Pan, W., Lyu, M., Hwang, K.S., Ju, M.Y., Shi, H.B.: A neuro Fuzzy Visual Servoing Controller for an Articulated Manipulator. IEEE Access. **6**, 3346–3357 (2018)
5. Yesim, O., Okyay, K.: Control of a direct drive robot using fuzzy spiking neural networks with variable structure systems-based learning algorithm. Neurocomputing. **149**, 690–699 (2015)
6. Sabahi, K., Ghaemi, S., Liu, J., Badamchizadeh, M.A.: Indirect predictive type-2 fuzzy neural network controller for a class of nonlinear input - delay systems. ISA Trans. **71**, 185–195 (2017)
7. Wai, R.J., Chen, P.C.: Robust Neural-Fuzzy-Network Control for Robot Manipulator Including Actuator Dynamics. IEEE Trans. Ind. Electron. **53**(4), 1328–1349 (2006)
8. Wai, R.J., Lin, Y.W.: Adaptive Moving-Target Tracking Control of a Vision-Based Mobile Robot via a Dynamic Petri Recurrent Fuzzy Neural Network. IEEE Trans. Fuzzy Syst. **21**(4), 688–701 (2013)
9. Wang, Y.C., Chien, C.J., Teng, C.C.: Direct Adaptive Iterative Learning Control of Nonlinear Systems Using an Output-Recurrent Fuzzy Neural Network. IEEE Transaction on systems, Man, and cybernetics – part b: Cybernetics. **34**(3), 1348–1359 (2004)
10. Lin, F.J., Shieh, P.H.: Recurrent RBFN-Based Fuzzy Neural Network Control for X-Y-Θ Motion Control Stage Using Linear Ultrasonic Motors. IEEE Trans. Ultrason. Ferroelectr. Freq. Control. **53**(12), 2450–2464 (2006)
11. Lin, F.J., Sun, I.F., Yang, K.J., Chang, J.K.: Recurrent Fuzzy Neural Cerebellar Model Articulation Network Fault-Tolerant Control of Six-Phase Permanent Magnet Synchronous Motor Position Servo Drive. IEEE Trans. Fuzzy Syst. **24**(1), 153–167 (2016)
12. Lin, F.J., Huang, P.K., Chou, W.D.: Recurrent-Fuzzy-Neural-Network-Controlled Linear Induction Motor Servo Drive Using Genetic Algorithms. IEEE Trans. Ind. Electron. **54**(3), 1449–1461 (2007)
13. Dehghan, S.A.M., Danesh, M., Sheikholeslam, F., Zekri, M.: Adaptive force–environment estimator for manipulators based on adaptive wavelet neural network. Appl. Soft Comput. **28**, 527–540 (2015)
14. Wei, S., Wang, Y., Zuo, Y.: Wavelet neural networks robust control of farm transmission line deicing robot manipulators. Computer Standards & Interfaces. **34**, 327–333 (2012)
15. Khan, M.M., Mendes, A., Zhang, P., Chalup, S.K.: Evolving multi-dimensional wavelet neural networks for classification using Cartesian Genetic Programming. Neurocomputing. **247**, 39–58 (2017)
16. Fayez, F.M.E.S., Khaled, A.A.: Adaptive Nonlinear Disturbance Observer Using a Double-Loop Self-Organizing Recurrent Wavelet Neural Network for a Two-Axis Motion Control System. IEEE Trans. Ind. Appl. **54**(1), 764–786 (2018)
17. Lin, F.J., Hung, Y.C., Ruan, K.C.: An Intelligent Second-Order Sliding-Mode Control for an Electric Power Steering System Using a Wavelet Fuzzy Neural Network. IEEE Trans. Fuzzy Syst. **22**(6), 1598–1611 (2014)
18. Wu, X., Wang, Y.N., Dang, X.J.: Robust adaptive sliding-mode control of condenser-cleaning mobile manipulator using fuzzy wavelet neural network. Fuzzy Sets Syst. **235**, 62–82 (2014)
19. Rahib, H.A., Okyay, K.: Fuzzy Wavelet Neural Networks for Identification and Control of Dynamic Plants—A Novel Structure and a Comparative Study. IEEE Trans. Ind. Electron. **55**(8), 3133–3140 (2008)
20. Tsai, C.H., Chuang, H.T.: Deadzone compensation based on constrained RBF neural network. Journal of the Franklin Institute. **341**, 361–374 (2004)
21. He, W., Dong, Y., Sun, C.: Adaptive neural network control of unknown nonlinear affine systems with input deadzone and output constraint. ISA Trans. **58**, 96–104 (2014)
22. Han, S.I., Lee, J.: Finite-time sliding surface constrained control for a robot manipulator with an unknown deadzone and disturbance. ISA Trans. **65**, 307–318 (2016)
23. Selmic, R., Lewis, F.L.: Deadzone compensation in motion control systems using neural networks. IEEE Trans. Autom. Control. **45**(4), 602–613 (2000)
24. Abiyev, R.H., Kaynak, O.: Fuzzy Wavelet Neural Networks for Identification and Control of Dynamic Plants—A Novel Structure and a Comparative Study. IEEE Trans. Industrial Electronics. **55**(8), 3133–3140 (2008)
25. Lewis, F.L., Tim, K., Wang, L.Z., Li, Z.X.: Deadzone compensation in motion control systems using adaptive fuzzy control system. IEEE Trans. Control Syst. Technol. **7**(6), 731–742 (1999)
26. Slotine, J.J.E., Li, W.: Applied Nonlinear Control. Prentice – Hall, Hoboken (1991)

Xuan Quynh Nguyen received the B.S. degree in Automation Engineering from best Military Technical Academy, Vietnam, in 2009.He received M.S.in Automation Engineering from Military Technical Academy, Vietnam, in 2011. He is currently working toward the Ph.D degree in Intelligent Control at college of Electrical and Information Engineering, Hunan University, Changsha, China, 410,082. He is working at College of Electrical technical technology, Hanoi University of Industry, Hanoi, Vietnam. His research interests include robot control, neural network, applications and robot manipulators, intelligent control.

Yaonan Wang received the B.S. degree in computer engineering from East China Science and Technology University (ECSTU), Fuzhou, China, in 1981, and the M.S. and Ph.D. degrees in Electrical Engineering from Hunan University, Changsha, China,in 1990 and 1994, respectively. He was with ECSTU from 1981 to 1994. He was a Post-Doctoral Research Fellow with the National University of Defense Technology, Changsha, from 1994 to 1995, a Senior Humboldt Fellow in Germany from 1998 to 2000, and a Visiting Professor with the University of Bremen, Bremen, Germany, from 2001 to 2004. He has been a Professor with Hunan University since 1995. His current research interests include robot control, intelligent control and information processing, industrial process control, and image processing

Vu Thi Yen received the B.S. and M.S. degree in Automation Engineering from Thai Nguyen University in 2008 and 2011 respectively. She is currently working toward the Ph.D degree in Intelligent Control at College of Electrical and Information Engineering, Hunan University, Changsha, China, 410,082. His research interests include Industrial robot, fuzzy logic, neural network and nonlinear system.